Cell, Vol. 104, 791–800, March 9, 2001, Copyright ©2001 by Cell Press

Structural Basis for the Inhibition of Caspase-3 by XIAP

Stefan J. Riedl,* Martin Renatus,* Robert Schwarzenbacher,* Qiao Zhou,* Chaohong Sun,† Stephen W. Fesik,† Robert C. Liddington,* and Guy S. Salvesen*‡
*The Program in Apoptosis and Cell Death Research
The Burnham Institute
10901 North Torrey Pines Road
La Jolla, California 92037
†Pharmaceutical Discovery Division
Abbott Laboratories
Abbott Park, Illinois 60064

Summary

The molecular mechanism(s) that regulate apoptosis by caspase inhibition remain poorly understood. The main endogenous inhibitors are members of the IAP family and are exemplified by XIAP, which regulates the initiator caspase-9, and the executioner caspases-3 and -7. We report the crystal structure of the second BIR domain of XIAP (BIR2) in complex with caspase-3, at a resolution of 2.7 Å, revealing the structural basis for inhibition. The inhibitor makes limited contacts through its BIR domain to the surface of the enzyme, and most contacts to caspase-3 originate from the N-terminal extension. This lies across the substrate binding cleft, but in reverse orientation compared to substrate binding. The mechanism of inhibition is due to a steric blockade prohibitive of substrate binding, and is distinct from the mechanism utilized by synthetic substrate analog inhibitors.

Introduction

The initiation and execution phases of apoptosis are both dependent on caspases, cytosolic cysteine proteases that cleave at Asp residues in their target substrates (Thornberry and Lazebnik, 1998). Caspase-8 initiates the extrinsic apoptotic pathway by integrating apoptotic signals transduced by cell surface death receptors (Krammer, 2000). Caspase-9 initiates the intrinsic apoptotic pathway to delete superfluous cells of the developing mammalian nervous system, and also in response to cellular damage (Nicholson, 1999). Both initiator caspases converge on the activation of the executioner caspases-3 and -7, which together cleave the many protein substrates that define the effector arm of apoptosis (Nicholson, 1999). The critical role of these caspases in transmitting death signals is underscored by the results of gene ablation experiments in mice where the phenotypes are very gross, evidently antiapoptotic, and vary from early embryonic lethality (caspases-7 and -8) to perinatal lethality (caspases-3 and -9) (Kuida et al., 1996, 1998; Hakem et al., 1998; Varfolomeev et al., 1998; Zheng et al., 1999). The structural basis of caspase activity is founded on atomic resolution structures of caspases-1, -3, -7, and -8 bound to substrate-analog peptidyl inhibitors (Walker et al., 1994; Wilson et al., 1994; Rotonda et al., 1996; Mittl et al., 1997; Blanchard et al., 1999; Watt et al., 1999; Wei et al., 2000). Substrates bind in an extended conformation to specificity pockets on the surface of the enzymes, and the scissile peptide bond is positioned close to the catalytic Cys. The subsite interactions observed in the crystal structures generally explain the selectivity of each caspase for its preferred substrates discovered by peptide mapping approaches (Thornberry et al., 1997; Stennicke et al., 2000).

The activity of caspases can be ablated by natural inhibitors. Indeed, viruses have adopted a successful strategy to control the apoptotic response of the host to viral infection by elaborating proteins that directly inhibit caspases. For example, the poxvirus inhibitor CrmA rapidly inactivates caspases-1 and -8, and the baculovirus inhibitor p35 rapidly inhibits an even wider profile of caspases (reviewed in Ekert et al., 1999). In each case, the target site on the inhibitor is in a well-defined sequence that satisfies the substrate binding requirements of the target caspases, and the mechanism appears similar to substrate hydrolysis, with the important exception that the enzyme active site is trapped during the reaction (Zhou et al., 1997, 1998). No homologs of p35 have yet been found in animals, and so far no animal homologs of CrmA have been found to target caspases. Animals have adopted another protein family to regulate caspase activity, namely the inhibitor of apoptosis proteins (IAPs).

The IAP family is characterized by a conserved module known as the BIR domain, and proteins containing this module have now been found throughout the eukaryotic kingdoms (Uren et al., 1998). Six human IAPs have been discovered, and at least four of them have been reported to directly inhibit caspases. They regulate apoptosis by preventing the action of the central execution phase, through direct inhibition of the executioner caspases-3 and/or -7. In addition, they prevent initiation of the intrinsic (postmitochondrial) apoptotic pathway by direct inhibition of the apical caspase-9. Human XIAP (Deveraux et al., 1997), cIAP1, and cIAP2 (Roy et al., 1997; Deveraux et al., 1998) can inhibit caspases-3, -7, and -9, but not caspases-1, -6, or -8. MLIAP/Livin shows weak inhibition of caspase-3, but more robust inhibition of caspase-9 (Kasof and Gomes, 2000; Vucic et al., 2000).

Dissection of XIAP reveals that the caspase-3/7 inhibitory segment is distinct from the caspase-9 inhibitory region. As previously demonstrated (Takahashi et al., 1998; Sun et al., 1999), the caspase-3 and -7 inhibitory function of XIAP can be traced to residues 163–240 of the 497 residue protein, a region that encompasses the second BIR domain, and an N-terminal extension, residues 124–162 (a combination defined here as BIR2), whereas a region encompassing the third BIR domain (residues 252–356) inhibits caspase-9 (Deveraux et al.,

‡To whom correspondence should be addressed (e-mail: gsalvesen@burnham.org).

Table 1. Summary of Crystallographic Analysis

	Native (λ = 1.08 Å)	Peak (λ = 1.282 Å)	Edge (λ = 1.283 Å)	Remote (λ = 1.181 Å)
Data set				
Resolution (Å)	2.7	2.8	2.8	2.8
Number of reflections				
Measured	174,633	84,386	84,839	81,987
Unique	27,119	23,991	24,035	23,817
Percent observed	99.4 (99.3)	95.8 (91.3)	95.9 (91.5)	96.4 (95.7)
R_{merge} (%)[a]	6.2 (42.4)	6.6 (42.3)	6.5 (46.7)	6.2 (45.4)
MAD Phasing		20 to 2.8 Å		
Figure of merit		38.6		
Space group	$P2_12_12_1$			
a, b, c	70.5, 95.5, 144.2			
Refinement				
Number of reflections	27,070			
Number of atoms				
non solvent	5,669			
solvent molecules	12			
R_{cryst}[b]/R_{free}[c]	24.84/27.76			
Stereochemical deviations				
distances	0.009 Å			
angles	1.30 degree			

[a] $R_{merge} = \Sigma|I - \langle I\rangle|/\Sigma I$, where I is the observed intensity and $\langle I\rangle$ is the average intensity from multiple observations of symmetry-related reflections, the value in parentheses correspond to the highest resolution shell.
[b] $R_{cryst} = \Sigma|(Fobs) - (Fcalc)|/\Sigma(Fobs)$.
[c] R_{free} = same as R_{cryst} but comprises a test set (5% of total reflections), which was not used in model refinement.

1999; Sun et al., 2000). BIR2 inhibits caspases-3 and -7 with apparent binding constants in the nanomolar range, accounting for the tight binding of the parent protein.

The BIR domain is a compact 70 residue zinc finger comprising 3 β strands and 4 α helices, characterized by the conservation of critical Cys and His residues that coordinate the zinc atom (Hinds et al., 1999; Sun et al., 1999; Chantalat et al., 2000; Muchmore et al., 2000; Verdecia et al., 2000). In addition to binding caspases, BIR domains can also interact with the protein Smac (Du et al., 2000) (also known as DIABLO [Verhagen et al., 2000]) to antagonize caspase binding, and thereby promote apoptosis. The structures of BIR3/Smac complexes have been solved (Liu et al., 2000; Wu et al., 2000), but the mode of inhibition of caspases by IAPs was previously unknown. To determine the mechanism, we have performed detailed kinetic analysis of the interaction of BIR2 with caspases-3 and -7, and obtained the crystal structure of caspase-3 in complex with BIR2.

Results and Discussion

Crystal Structure of the BIR2/Caspase-3 Complex

Crystals of the BIR2/caspase-3 complex (Table 1) contain two caspase catalytic domains and two BIR2 domains per asymmetric unit (Figure 1). Each caspase catalytic domain is composed of a large and a small subunit, cleaved at the intradomain site, IETD. The two caspase-3 catalytic domains are structurally identical (RMS deviation for Cα positions = 0.43 Å). They form a functional dimer with two active sites, and the overall structure is very similar to other caspase-3 structures (Rotonda et al., 1996; Mittl et al., 1997). The caspase-3 mutant used in this study contained the natural 28 residue N-terminal propeptide. No density could be found for those residues, indicating that they are highly flexible. Each catalytic site is occupied by one BIR2 molecule, resulting in a 95 kDa complex with dimensions of 100 Å $\times$ 60 Å $\times$ 60 Å. Despite different packing interactions, the structures of both inhibitor molecules in the asymmetric unit are almost identical, with the exception of a 10 residue loop distal to the BIR/caspase interaction site. The core BIR domain (residues 163–240) closely resembles its solution structure (Sun et al., 1999) and other BIR domains (Hinds et al., 1999; Sun et al., 1999; Chantalat et al., 2000; Muchmore et al., 2000; Verdecia et al., 2000), indicating that this type of domain maintains its rigid state in the presence of its cognate ligand. Yet the N-terminal region (residues 124–162) differs. This region is mainly flexible in the BIR2 solution structure, while it is well defined in the complex. BIR2 in complex with caspase-3 has two additional helical turn regions (residues 150–152 and 158–161) not observed in solution, demonstrating that complex formation induces conformational stabilization of the N-terminal region.

Binding of the Inhibitor

The inhibitor binds across the caspase-3 substrate binding site in an elongated manner, leaving a footprint of 12 $\times$ 35 Å^2. The interactions between both molecules comprise about 200 non-hydrogen atoms, excluding a surface of 2600 Å^2 that involves three interaction sites. Parts of the globular BIR domain and residues upstream (the "sinker") provide a core of one binding motif, while the N-terminal helix acts as the core of the second binding unit (the "hook") (Figure 2A).

The first interaction site involves the hook of BIR2 (residues 138–146). A hydrophobic cluster made by the caspase-3 residues L290, Y338, W340, and F381h engages the BIR2 residues L140, V146, and L141 (Figure 2C). A network of hydrogen bonds from T143, G144, and V146 also contribute to the interaction. The impor-

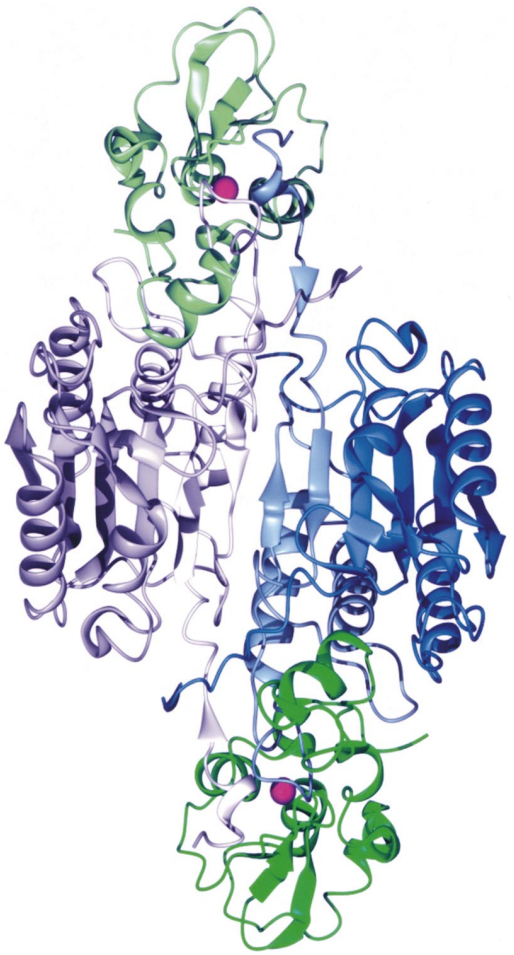

Figure 1. Standard View of Caspase-3 with BIR2 Domains Bound

The asymmetric unit is composed of two caspase-3 catalytic domains (blue and purple), each one binding a BIR2 molecule (green). The large and small subunits of each catalytic domain are shaded differently. Each BIR2 molecule constitutes a globular domain and an N-terminal extension occupying the catalytic edge of each caspase. The pink sphere at the core of each BIR domain is the zinc atom.

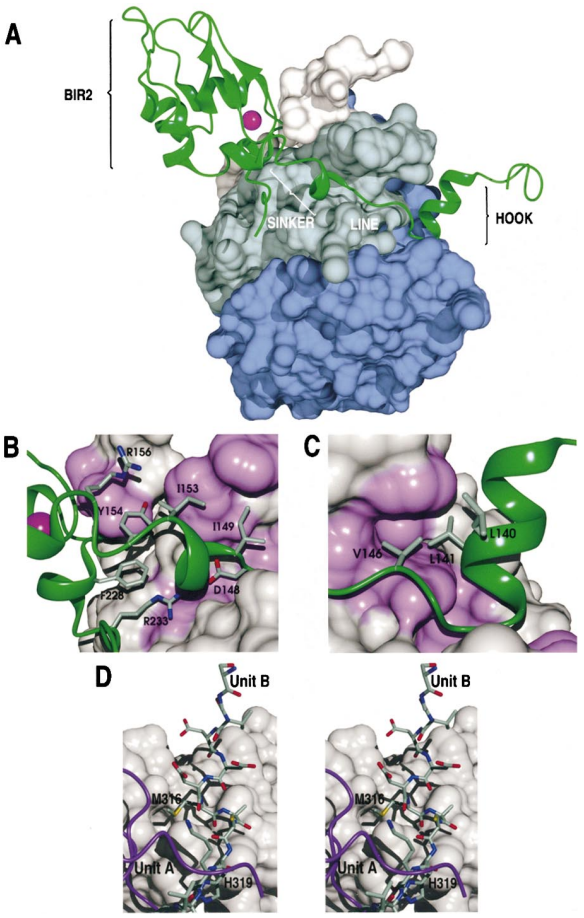

Figure 2. Details of the Contacts between BIR2 and Caspase-3

(A) Overview of the inhibited caspase. The chain trace of BIR2 is shown in green, running from the right (N-terminal) to the left (C-terminal) with the hook, line, sinker, and BIR substructures identified. It binds backward compared to the usual direction of protein substrates. Contacts are made with both the large caspase-3 subunit (dark blue), the small caspase-3 subunit (light blue) of the inhibited caspase-3 catalytic domain (unit A), and also with a short stretch of the adjacent caspase-3 domain (unit B, gray).

(B) Interactions between caspase-3 and the sinker and BIR domain. The major interactions from the sinker are hydrophobic, with two isoleucine side chains (I149 and I153), Y154 and the stem of R156 (gray sticks), attached to hydrophobic residues of the 381 loop of caspase-3 (purple patch). Two hydrophobic interactions from BIR side chains contribute F228 and the stem of R233, with a hydrophobic patch underneath the main chain of BIR2. H bonds are donated by D148 from the sinker.

(C) The N-terminal hook comprises the first major binding unit. Two leucine side chains (L140 and L141) and V146 (all in gray sticks) in the hook form an interaction with a hydrophobic patch (purple) on the surface of caspase-3, helping to align the helix.

(D) Interaction of caspase unit B with BIR unit A, with the surface representing the BIR domain. The N-terminal residues of the small caspase subunit of unit B (sticks) interface with the BIR unit A (gray surface). M316 sits in a hydrophobic pocket at the BIR-caspase interface close to the zinc motif, and H319 forms an H bond with N226 of the BIR domain.

tance of the hydrophobic interactions is demonstrated by the BIR2 mutation L141A, which abolishes inhibitory activity (Sun et al., 1999).

From the hook, the two peptide bonds on either side of the V147 Cα (the "line") stretch across the caspase substrate binding cleft, leading to the "sinker" just before the globular BIR domain. The second major interaction site comprises the sinker (residues 148–156), and part of the BIR domain itself, which make both hydrophobic and H-bond interactions (Figure 2B). The caspase-3 residues F381b and F381d and the BIR2 residues I149 and I153 form a hydrophobic cluster. The mutation of I149 reduces the activity of BIR2, although the effect is less drastic than the mutation of L141 (Sun et al., 1999). A key residue is D148, which provides not only H bonds to the caspase (R341, S343, W348, and F381b), but also forms a buried salt bridge with R233 at the C terminus of the BIR domain. This interaction is likely to be critical for locking the BIR domain against the side of caspase-3, which would explain the total loss of inhibitory activity of a D148A mutant (Sun et al., 1999).

The major direct contacts from the BIR domain are from the two residues on either side of the final Zn-

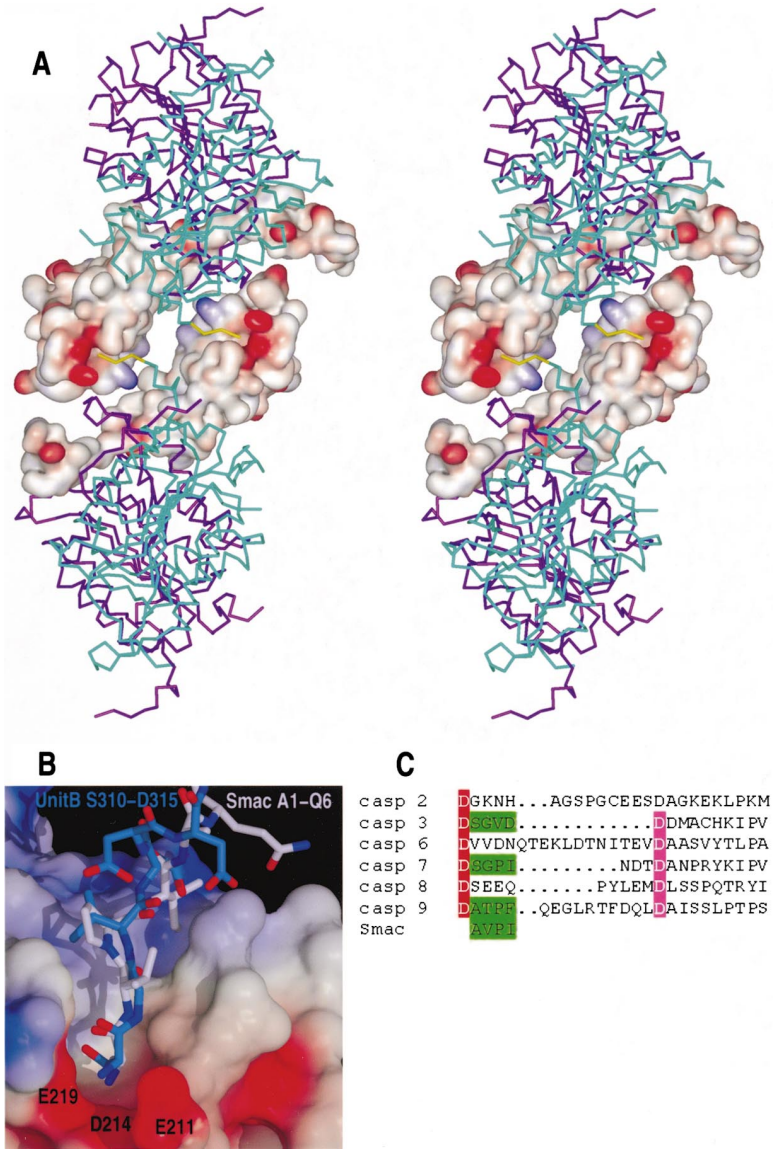

Figure 3. Interactions with the Smac Pocket

(A) Cross-domain interactions of caspase-3 with BIR2 stabilize the N terminus of the caspase-3 small subunit. Two adjacent BIR2 domains are rendered with an electrostatic surface, and the associated caspase-3 large subunits (purple) and small subunits (cyan) are shown in Cα trace. The N-terminal four residues of the caspase small subunits in the crystal all lie in a pocket on the adjacent BIR domain. This pocket is topologically equivalent to the Smac pocket of BIR3. The interacting portions are highlighted in yellow.

(B) BIR2 and BIR3 domains have been superimposed, and the BIR2 surface rendered to show charged residues. The N terminus of the small subunit of caspase-3 (blue) matches well with the Smac N terminus (white). The N terminus of the caspase small subunit is surrounded by the acidic patch comprising E211, D214, and E219.

(C) Cleavage sites in the interdomain linker of human caspases are identified. The primary caspase processing sites are highlighted in red, and the four residues compatible with binding in the Smac pockets of BIR domains are highlighted in green. The secondary cleavage site is highlighted in purple. Cleavage at the secondary site, which occurs during apoptosis, would shorten the caspase-3, -7, and -9 small subunit N-terminals such that they would not be long enough to stretch across to the Smac pocket of adjacent BIR domains.

coordinating cysteine, C227, which contact residues 316–318 at the N terminus of the small subunit of the second catalytic domain of the caspase dimer (Figure 2D).

The N terminus of the small caspase-3 subunit is disordered in all previous structures, but in the structure reported here, we traced the polypeptide chain through to its N terminus. This is due to the stabilizing interactions with a symmetry-related molecule in the crystal lattice (Figure 3A). Inspection of this interaction revealed that the N terminus binds into the putative Smac pocket of BIR2.

Interactions in the Smac Pocket

Smac is a mitochondrial protein that has been demonstrated to accelerate apoptosis by sequestering IAPs so that they can no longer inhibit caspases (Du et al., 2000; Verhagen et al., 2000), and the interaction site has been traced to a pocket on BIR3 that accepts the Smac N terminus (Liu et al., 2000; Wu et al., 2000). Superimposition of the BIR3/Smac structure with BIR2 reveals a topologically equivalent pocket with strong chemical similarities (Figure 3B). The pocket in BIR2 is occupied by the N terminus of the adjacent caspase-3 small subunit. The three N-terminal residues of Smac and caspase-3 superimpose well. In both structures, the positively charged N-terminal amino group is sandwiched between two residues, D214 and E219 (BIR2) or E314 and Q319 (BIR3). This ionic interaction is followed by a short antiparallel β-sheet-like structure. Residues V312 of caspase-3 and P3 of Smac occupy a similar position (Figure 3B). Interestingly, an alignment of activation cleavage sites in caspases (Figure 3C) shows that the four N-terminal residues of the small subunit of caspases-3, -7 and -9 are sterically capable of binding to the Smac site. Interestingly, caspases-2, -6 and -8, which are not inhibited by IAPs, lack similar sequences.

The BIR-antagonist action of Smac has been suggested to be due to an overlap with caspase interaction sites (Liu et al., 2000; Wu et al., 2000). In modeling the

trimolecular complex of Smac/BIR/caspase based on the Smac/BIR3 structures we can see how steric clashes from Smac would preclude caspase-3 from binding to BIR2. However, it is not clear how simple oligopeptides mimicking the Smac N terminus (Srinivasula et al., 2000) would accomplish this, since the Smac interaction site is separate from the BIR2 interaction site (Figure 3A).

Specificity of BIR2 for Caspases

The interactions demonstrated in Figure 2 account for the inhibition of caspase-3 and probably also for its closest relative, caspase-7. However, no other known caspases are inhibited (Deveraux et al., 1997, 1999). To understand the structural basis of this selectivity, we superimposed the structures of caspase-8 (Blanchard et al., 1999; Watt et al., 1999) and caspase-9 (M. R., unpublished data) onto the BIR2/caspase-3 structure. The lack of binding to caspase-8 and -9 is readily explained by the absence of the hydrophobic pattern of the 381 loop, such that important interactions with the hook and sinker of BIR2 cannot form. On the other hand, the third BIR domain of XIAP (BIR3) selectively inhibits caspase-9 (Deveraux et al., 1999; Sun et al., 2000), and so we modeled the interaction of caspase-9 and BIR3 based on our structure of the BIR2/caspase-3 complex. BIR3 could be readily docked to caspase-9 in the same orientation of the BIR2/caspase-3 complex, but changes in the orientation of the C-terminal helix of BIR3 would have to be made to explain the critical interactions predicted by mutagenesis experiments (Sun et al., 2000). Moreover, inhibition of caspase-9 does occur in the absence of a region of BIR3 equivalent to the hook of BIR2 (Sun et al., 2000). Thus, differences must exist in the binding mode of BIR3 and caspase-3, but these can, in principle, be accommodated within the frame of the BIR2/caspase-3 orientation.

Mechanism of Inhibition

The first step in peptide bond hydrolysis is acylation of a protein carbonyl. The hook adopts a structure that precludes the first step; all the potential carbonyls are too far away to be attacked by the catalytic Cys of caspase-3 (Figure 4A), and a steric blockade is imposed on the active site. This explains why the catalytic mutant of caspase-3 binds, since the natural catalytic Cys does not participate in the interaction. In addition, BIR2 binds in a reverse orientation with respect to substrates such that even if acylation occurred, hydrolysis by the normal mechanism would be impossible. The structure also explains why caspase-3 treated by Z-VAD-fmk is unable to bind BIR2 (Figure 4C and Sun et al., 1999), since there would be severe clashes with the bound inhibitor, displacing the hook and line of BIR2.

These molecular interactions nicely explain the inhibition kinetics between BIR2 and caspases. Both caspase-3 and -7 are tightly bound, with caspase-7 being more efficiently inhibited (Table 2). The different inhibition constants (K_i) are determined primarily by association rates (k_{on}), with BIR2 reacting significantly faster with caspase-7 than with caspase-3. The dissociation rates (k_{off}) were estimated as a product of K_i and k_{on}, assuming a simple reversible interaction. The estimated dissociation rate agreed well with an experimentally derived value ($k_{off} = 1.2 \times 10^{-3}\ s^{-1}$) confirming the simple reversibility of the interaction (see Experimental Procedures). The complex between BIR2 and caspase-3 or -7 was observed under nondenaturing conditions (Figure 4C). Complexes of caspase-3 or -7 with BIR2 are dissociated to their constituent subunits in SDS-PAGE. No cleavage of the BIR2 protein was observed in any of these interactions, as BIR2 was seen to remain as a single 17 kDa band in SDS-PAGE, indicating that the catalytic apparatus of caspases is not required for inhibition by BIR2. These data show BIR2 to be a rapid, tight binding, noncovalent, and fully reversible inhibitor of caspase-3 and -7, consistent with the lack of covalent interactions between the inhibitor and enzyme revealed in the structure.

Differences between BIR2 and Peptide Inhibitors

Although synthetic peptidyl inhibitors of caspase-3 (Rotonda et al., 1996; Mittl et al., 1997) and the hook-line-sinker of BIR2 both occupy the active site, the modes of interaction and mechanism of inhibition are very different. The peptidyl inhibitors (such as DEVD-aldehyde and DEVD-fmk) bind in the same way as substrates, and utilize the catalytic function of caspases to achieve binding, acting as transition state analogs or covalent modifiers. They fully occupy the substrate binding sites. The arrangement of the hook not only precludes the approach of the BIR2 chain to the catalytic center, but also impedes occupancy of the S1, S2, and S3 substrate recognition sites. In the DEVD structures, an Asp side chain occupies the S1 pocket, and this is replaced in the BIR2 structure by a water molecule. The S2 pocket is blocked by a caspase side chain in the BIR2 complex (Figure 4B). Here, the side chain of Y338 occupies the volume corresponding to the S2 site due to an 85° rotation around $\chi 1$ compared to the DEVD-bound structures (Rotonda et al., 1996; Mittl et al., 1997). The rotation of Y338 implies that either the ground state of the enzyme contains a blocked S2 subsite that opens during substrate binding, or that the interaction of BIR2 forces Y338 down to block the preexisting pocket. Interestingly, Y338 and its neighbor F381h are the only nonsurface caspase side chains that are altered by BIR2 binding. The only interaction that can be considered equivalent between the two modes of inhibitor binding is within the S4 subsite, which in caspase-3 and -7 is highly specific for Asp side chains (Thornberry et al., 1997). In the crystal structure, D148 of BIR2 occupies the S4 pocket (Figure 4B), which is occupied by a topologically equivalent Asp in the DEVD structures.

Overall, the solution adopted by BIR2 to the problem of specifically inhibiting caspase-3 and -7 bears almost no relationship to the mechanism of substrate analogs. Interestingly, it is also much more selective, since the analogs react with almost all caspases (Garcia-Calvo et al., 1998), whereas BIR2 is only known to inhibit caspase-3 and its close relative, caspase-7 (Deveraux et al., 1999).

Comparison with Other Protease Inhibitors

There are at least two properties of BIR2 that restrain cleavage: its reverse binding and the prevention of approach to the catalytic center. The overall inhibitory con-

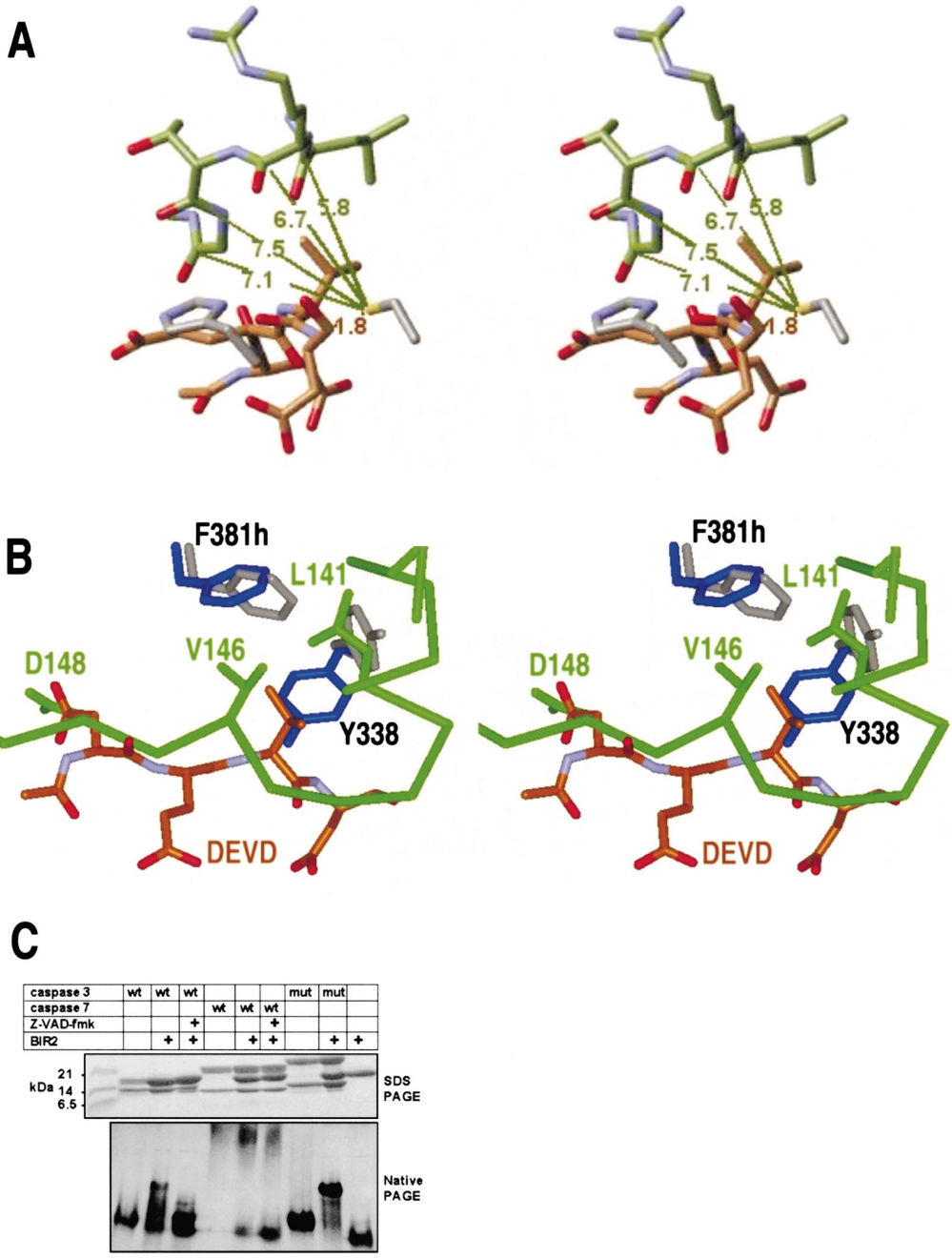

Figure 4. Mechanism of Inhibition

(A) The BIR2 hook region (green) is superimposed on the structure of the substrate analog DEVD-aldehyde (in brown) bound to caspase-3, with its catalytic residues H237 and C285 shown in gray (1PAU; Rotonda et al., 1996). The distance from Sγ of the catalytic Cys to the carbonyl carbon of the substrate analog is 1.8 Å, but the closest approach of a BIR2 carbonyl is 5.8 Å, well out of the reach of atomic interactions.

(B) Focus on the substrate binding region of caspase-3, and comparison of DEVD-aldehyde and BIR2 binding interactions. The trace of BIR2 (green) is superimposed on the caspase-3 structure with DEVD-aldehyde (brown) bound. Two caspase-3 side chains (Y338 and F381h) that occupy different rotamers in the two complexes are highlighted. In blue is their position in the BIR2 structure, and in gray is their position in the DEVD-aldehyde structure. To the left of the panel the side chain of D148 of BIR2 and the topologically equivalent P4 Asp residue of DEVD-aldehyde are shown.

(C) The interaction between BIR and caspase-3 or -7 was observed by nondenaturing and SDS-PAGE. A 1.2-fold molar excess of BIR2 was incubated with wild-type (wt) caspase-3 or caspase-7, or C285A caspase-3 (mut), and complex formation visualized as a gel shift in nondenaturing PAGE. Binding of BIR2 could be prevented by pretreating caspase-3 with Z-VAD-fmk. The complex was dissociated in SDS-PAGE (top panel), and no cleavage of BIR2 was observed.

Table 2. Inhibition Parameters of BIR2 on Caspase-3 and Caspase-7

	K_i (M)	k_{on} (M^{-1} s^{-1})	Calculated k_{off} (s^{-1})
Caspase-3	9.7 ($\pm$5.0) $\times$ 10^{-10}	2.5 ($\pm$1.0) $\times$ 10^{6}	2.4 $\times$ 10^{-3}
Caspase-7	1.0 ($\pm$0.4) $\times$ 10^{-10}	1.4 ($\pm$0.5) $\times$ 10^{7}	1.4 $\times$ 10^{-3}

K_i and k_{on} values are given as $\pm$ standard deviation of three data sets.

formation is summarized in Figure 5. Almost all natural protease inhibitors prevent access of substrates to the proteases' catalytic centers by steric hindrance, and have adopted a range of divergent mechanisms to accomplish this goal. However, the BIR2 mechanism appears unique. Members of the kunitz and kazal family of serine protease inhibitors, for example, bind in the same orientation as substrates (Bode and Huber, 1991). Inhibition is created by rigidity of the frame, which does not allow approach to the transition state (Read and James, 1986). The TIMPs inhibit their target matrix metalloproteases by occupying the binding cleft in a similar substrate-like manner, but catalysis is prevented by coordination of the critical zinc of the protease by an inhibitor side chain (Bode and Huber, 2000). Other inhibitors of serine proteases, notably the serpins, allow the initial step in cleavage, but trap the acyl enzyme intermediate (Huntington et al., 2000). Indeed, this may explain the mechanism of the caspase inhibitor CrmA (which is a serpin) and possibly also baculovirus p35, since both appear to require cleavage for their function. However, trapping of acyl enzymes by suicide inhibition, as it is sometimes called (Patston et al., 1991), applies only to serpins and p35, and other inhibitor families have adopted ingenious strategies for protease inhibition.

The cystatin family of cysteine protease inhibitors function in part by using a similar mechanism to that of BIR2, as they do not conform to the substrate pockets and place a structure distant from the catalytic center (Stubbs et al., 1990). Yet the cystatins still interact in the same orientation as substrates. The closest similarity among previously known mechanisms is with some thrombin inhibitors, exemplified by the medical leech-derived protein hirudin. The N terminus of hirudin lies in thrombin's S1 pocket and the chain proceeds in a reverse orientation to a second site on the surface of the enzyme, the exosite, that tightens the inhibitory interaction (Rydel et al., 1990), somewhat similar in principle to the BIR interaction with caspase-3.

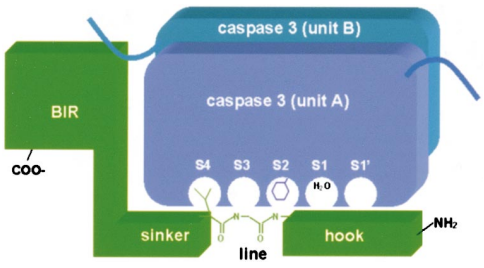

Figure 5. Diagrammatic Representation Illustrating the Topological Contacts in BIR2-Inhibited Caspase-3

The substrate pockets designated by "S" have been defined on the basis of caspase structures bound to peptidyl inhibitors. They are mostly unoccupied by BIR2, with the exception of S4. The most important inhibitory interaction comes from the hook, which ablates catalytic activity by sterically hindering substrate access. The sinker and BIR domain help to stabilize the complex, acting as exosite binding elements. The cross-unit interaction shown by the thin blue line may also help to stabilize the complex.

Perhaps the closest similarity between the BIR2 inhibitory mechanism and other known protein:protease interactions is seen in the zymogens of members of the papain family of cysteine proteases. These zymogens contain a fully formed active site that is blocked by the N-terminal propeptide (Turk et al., 2000). The prodomain contains a helix at the top of the catalytic site that continues through the protease specificity sites in reverse direction compared with substrates. Though the nature of the contacts and organization of the prodomain are completely different to BIR2, it is interesting that the two completely unrelated families of cysteine proteases have converged on a comparable mechanism for ablating activity. Of course, the papain family prodomains exist to regulate the activation of the enzymes, whereas BIR2 exists to ensure the inhibition of caspases, but the similarities are nonetheless intriguing.

Conclusions

The inhibition of caspase-3 by BIR2 demonstrates classic reversible tight binding kinetics, and this is explained by the noncovalent blocking of the active site by a novel structure, the helical hook. The hook is necessary, but not sufficient, since mutations in either the hook or the sinker eliminate inhibition (Sun et al., 1999). However, the hook-line-sinker substructures themselves are still not sufficient for inhibition, since a synthetic peptide spanning this region still does not inhibit caspase-3 (Sun et al., 1999). The BIR domain is required, presumably, to align and stabilize the main inhibitory interactions.

It is clear that the cell's solution to the problem of how to specifically inhibit caspases does not reside in the BIR domains, but rather in the interdomain segments between domains. The unique solution utilizes a large number of interactions, and abolishing even one of these can ablate inhibition. This information, and the molecular determinants of the interactions, will be useful in the design of drugs that can be used to antagonize IAP inhibition of caspases. For example, small molecules that bind the hook or sinker will be specific for antagonizing inhibition of caspase-3 and -7 without affecting caspase-9 inhibition. Such molecules would be exquisitely specific, and may be especially useful to facilitate caspase activity by extrinsic (caspase-8) pathway triggers in cancers where IAPs are overexpressed, without affecting other IAP-protein interactions.

Experimental Procedures

Recombinant Proteins

A region of XIAP that potently inhibits caspases-3 and -7 was generated by PCR from a pGEX construct containing the XIAP cDNA

(Takahashi et al., 1998). The fragments were ligated into the NdeI and XhoI sites of pET23b, resulting in a construct containing residues 124–240, plus a C-terminal His-6 tag, which was used to transform *E. coli* BL21(DE3)pLysS. Protein was expressed by induction with 0.4 mM IPTG for 4 hr at 30°C. The protein was purified on Ni-chelate Sepharose (Pharmacia) from the soluble fraction of sonicated cells. For crystallization, a BIR2 construct containing residues 124–240 (containing mutations C202A and C213G) was used (Sun et al., 1999). Active recombinant caspases-3 and -7 were produced in *E. coli* (Stennicke and Salvesen, 1999) and purified by Ni-chelate chromatography. The active concentrations were determined by titration with the irreversible caspase inhibitor Z-Val-Ala-Asp-fluoromethyl ketone (Z-VAD-fmk, Enzyme Systems Products) as previously described (Stennicke and Salvesen, 1999). The caspase-3 and -7 catalytic mutants (C285A) were constructed by overlap PCR (Stennicke et al., 1998). The catalytic mutants of caspases-3 and -7 were converted by treatment with a 0.01 molar ratio granzyme B for 15 min at 37°C, resulting in cleavage at the interdomain linker after IETD and IQAD, respectively.

Spectrophotometry and Spectrofluorometry

The caspase substrate Ac-Asp-Glu-Val-Asp-p-nitroanilide (Ac-DEVD-pNA) was purchased from Biomol and Z-Asp-Glu-Val-Asp-7-amino-4-trifluoromethyl-coumarin (Z-DEVD-AFC) was from Enzyme Systems Products. Assays using colorimetric pNA substrates (maximal absorbance at 405 nm) were performed on a SpectraMAX 340 plate reader coupled with SOFTMAX software (Molecular Devices, Sunnyvale, CA). Assays using fluorogenic substrates were carried out on Perkin-Elmer LS50B luminescence spectrometer coupled with the FL WinLab software (Perkin Elmer Corp) or fmax Fluorescence Plate Reader (Molecular Devices) at excitation wavelength 400 nm and emission wavelength 505 nm. All assays were thermostated at 37°C.

Inhibition Kinetics

Inhibition rates and equilibria were determined as previously described (Zhou and Salvesen, 2000). For dissociation kinetics, complexes were first formed by incubating the caspase with an excess of BIR2 in assay buffer at 100-fold above the eventual assay concentration, for sufficient time to ensure >99% complex formation. Following incubation, an aliquot was diluted into a large volume of assay buffer containing a large excess of substrate and the assay started immediately. The inhibitor was diluted to around its K_i, and the assay was followed until a new equilibrium rate was achieved for a period of time.

The integrated rate equation for the dissociation of equimolar complex (Morrison and Walsh, 1988) with a dissociation rate constant k_{off} is:

$$P = K \cdot E_0 \, (t - (1 - e^{-koff \cdot t}) / k_{off}) + P_0$$

where $K = k_{cat}\,[S]/(K_m + [S])$.

Kinetic data were analyzed either by linear or nonlinear regression as appropriate. The latter was performed with the aid of the computer program Kaleidagraph (Synergy Software).

SDS-PAGE and Nondenaturing PAGE

8%–18% linear acrylamide gradient PAGE was performed with a 2-amino-2-methyl-1,3-propanediol/glycine/HCL buffer system with or without SDS to resolve proteins (Bury, 1981). Samples for SDS-PAGE were boiled in SDS sample buffer containing 50 mM DTT for 5 min. Protein gels were stained with Coomassie blue.

Crystallization

The complex of processed caspase-3 C285A and BIR2 was formed by incubation of the two components for 5 min at 37°C with a 2-fold excess of inhibitor and purified by gel filtration in 10 mM HEPES, 100 mM NaCl, and 2 mM DTT (pH 7.6). After concentration to 8 mg/ml, the complex was quick frozen in 50 μl aliquots and stored at –80°C. The complex was crystallized by sitting drop vapor diffusion against 0.1 M sodium acetate and 1.8 M sodium formate (pH 5.2). A 9 μl portion of protein solution was mixed with an equal amount of reservoir solution. Crystals grew at 23°C within 5–10 days.

Data Collection and Structure Solution

A first, low resolution (4 Å) data set was collected from a frozen crystal (using 30% [v/v] glycerol for cryo protection) on an R-AXIS IV image plate mounted on a Rigaku rotating anode. Data were processed with DENZO and SCALEPACK (Otwinowski and Minor, 1997). Two caspase-3 molecules (search model 1PAU, [Rotonda et al., 1996]) were located in the asymmetric unit by molecular replacement using the program AmoRe (Navazza, 1994). Both rotational and translational searches gave clear peaks. After rigid body refinement within AmoRe, the R factor dropped to 42.6%. Analysis of the crystal packing revealed that the caspase-3 molecules form dimers identical to the ones seen in other crystal structures, strongly supporting this molecular replacement solution. No crystal contacts were found between the caspase dimers, suggesting that BIR2 was indeed present in the crystals. Yet, BIR2 gave no rotational solution in AmoRe using the NMR structure (Sun et al., 1999) as a search molecule, and electron density in the expected BIR binding region was difficult to interpret. We therefore utilized the BIR2 zinc atoms for MAD phasing.

Four data sets were collected at the SSRL (peak, inflection point and remote on beamline 9-2 and one native data set on beamline 7-1). Two zinc sites were found and MAD phases calculated with the program SOLVE (Terwilliger and Berendzen, 1999). The map was improved using DM (Collaborative Computational Project, 1994) and then used for model building. Phase combination of experimental phases with molecular replacement phases was not necessary because almost all BIR2 residues could be built (following the topology defined by the BIR2 solution structure) in this density. An initial model was refined in CNS (Brunger et al., 1998) (R_w/R_{free} = 35.6/39.6). After several cycles of model building in Main (Turk, 1992) and crystallographic refinement (simulated annealing and positional and temperature-factor refinement applying NCS constrains between the two catalytic units of caspase-3 and the two BIR2 molecules) in CNS (Brunger et al., 1998) using target parameters (Engh and Huber, 1991), the R factor dropped to R_{work}/R_{free} = 24.9/27.8.

The final model consists of two catalytic units of caspase-3 with two BIR2 inhibitors, and contains the following residues: 148–296 (large subunit) and 310–401 (small subunit) of caspase unit A, and residues 127–237 of the corresponding BIR2; residues 148–297 (large subunit) and 310–401 (small subunit) of caspase unit B, and residues 135–169 and 180–236 of its BIR2. Figures were prepared using the programs Dino (DINO: Visualizing Structural Biology [2001]; http://www.biozentrum.unibas.ch/~xray/dino), Spock (Christopher, J. A.; SPOCK: The Structural Properties Observation and Calculation Kit [program manual], The Center for Macromolekular Design, Texas A&M University, College Station, TX [1998]), WebLab Viewer Pro, and Raster 3D (Merritt and Murphy, 1994).

Acknowledgments

We thank Chris Froelich for providing granzyme B, Chao-Zhou Ni and Jose Maria De Pereda for help with crystal measurements, Laurie Bankston for preliminary experimental work and advice, Nuria Assa-Munt, Scott Snipas, and Kate Welsh for supplying protein for initial trials, and Quinn Deveraux, John Reed, and Henning Stennicke for helpful suggestions. Supported by grant AG15402 from the NIH. Portions of this research were carried out at the Stanford Synchrotron Radiation Laboratory, a national user facility operated by Stanford University on behalf of the U.S. DOE, Office of Basic Energy Sciences. The SSRL Structural Molecular Biology Program is supported by the DOE, Office of Biological and Environmental Research, and by the NIH, National Center for Research Resources, Biomedical Technology Programs, and the NIGMS.

Received February 8, 2001; revised February 22, 2001.

References

Blanchard, H., Kodandapani, L., Mittl, P.R.E., Di Marco, S., Krebs, J.F., Wu, J.C., Tomaselli, K.J., and Grütter, M.G. (1999). The three-dimensional structure of caspase-8: an initiator enzyme in apoptosis. Structure *27*, 1125–1133.

Bode, W., and Huber, R. (1991). Ligand binding: proteinase-proteinase inhibitor interactions. Curr. Opin. Struct. Biol. *1*, 45–52.

Bode, W., and Huber, R. (2000). Structural basis of the endoproteinase-protein inhibitor interaction. Biochem. Biophys. Acta *1477*, 241–252.

Brunger, A.T., Adams, P.D., Clore, G.M., Delano, W.L., Gros, P., Grosse-Kunstleve, R.W., Jiang, J.-S., Kuszewski, J., Nilges, N., Pannu, N.S., et al. (1998). Crystallography & NMR system (CNS): a new software suite for macromolecular structure determination. Acta Crystallogr. *D54*, 905–921.

Bury, A. (1981). Analysis of protein and peptide mixtures: evaluation of three sodium dodecyl sulphate-polyacrylamide gel electrophoresis buffer systems. J Chromatog. *213*, 491–500.

Chantalat, L., Skoufias, D.A., Kleman, J.P., Jung, B., Dideberg, O., and Margolis, R.L. (2000). Crystal structure of human survivin reveals a bow tie-shaped dimer with two unusual alpha-helical extensions. Mol. Cell *6*, 183–189.

Collaborative Computational Project (1994). The CCP4 suite: programs for protein crystallography. Acta Crystallogr. *D50*, 760–763.

Deveraux, Q., Takahashi, R., Salvesen, G.S., and Reed, J.C. (1997). X-linked IAP is a direct inhibitor of cell death proteases. Nature *388*, 300–304.

Deveraux, Q.L., Roy, N., Stennicke, H.R., Zhou, Q., Srinivasula, S.M., Alnemri, E.S., Salvesen, G.S., and Reed, J. (1998). IAPs block apoptotic events induced by caspase 8 and cytochrome C by direct inhibition of distinct caspases. EMBO J. *17*, 2215–2223.

Deveraux, Q.L., Leo, E., Stennicke, H.R., Welsh, K., Salvesen, G.S., and Reed, J.C. (1999). Cleavage of human inhibitor of apoptosis protein XIAP results in fragments with distinct specificities for caspases. EMBO J. *18*, 5242–5251.

Du, C., Fang, M., Li, Y., Li, L., and Wang, X. (2000). Smac, a mitochondrial protein that promotes cytochrome c-dependent caspase activation by eliminating IAP inhibition, Cell *102*, 33–42.

Ekert, P.G., Silke, J., and Vaux, D.L. (1999). Caspase inhibitors. Cell Death Differ. *6*, 1081–1086.

Engh, R.A., and Huber, R. (1991). Accurate bond and angle parameters for X-ray protein-structure refinement. Acta Crystallogr. *A47*, 392–400.

Garcia-Calvo, M., Peterson, E.P., Leiting, B., Ruel, R., Nicholson, D.W., and Thornberry, N.A. (1998). Inhibition of human caspases by peptide-based and macromolecular inhibitors. J. Biol. Chem. *273*, 32608–32613.

Hakem, R., Hakem, A., Duncan, G.S., Henderson, J.T., Woo, M., Soengas, M.S., Elia, A., de la Pompa, J.L., Kagi, D., Khoo, W., et al. (1998). Differential requirement for caspase 9 in apoptotic pathways in vivo. Cell *94*, 339–352.

Hinds, M.G., Norton, R.S., Vaux, D.L., and Day, C.L. (1999). Solution structure of a baculoviral inhibitor of apoptosis (IAP) repeat. Nat. Struct. Biol. *6*, 648–651.

Huntington, J.A., Read, R.J., and Carrell, R.W. (2000). Structure of a serpin-protease complex shows inhibition by deformation. Nature *407*, 923–926.

Kasof, G.M., and Gomes, B.C. (2000). Livin, a novel inhibitor-of-apoptosis (IAP) family member. J. Biol. Chem. *9*, 9.

Krammer, P.H. (2000). CD95's deadly mission in the immune system. Nature *407*, 789–795.

Kuida, K., Zheng, T.S., Na, S., Kuan, C.-y., Yang, D., Karasuyama, H., Rakic, P., and Flavell, R.A. (1996). Decreased apoptosis in the brain and premature lethality in CPP32-deficient mice. Nature *384*, 368–372.

Kuida, K., Haydar, T.F., Kuan, C.Y., Gu, Y., Taya, C., Karasuyama, H., Su, M.S., Rakic, P., and Flavell, R.A. (1998). Reduced apoptosis and cytochrome c-mediated caspase activation in mice lacking caspase *9*. Cell *94*, 325–337.

Liu, Z., Sun, C., Olejniczak, E.T., Meadows, R.P., Betz, S.F., Oost, T., Herrmann, J., Wu, J.C., and Fesik, S.W. (2000). Structural basis for binding of Smac/DIABLO to the XIAP BIR3 domain. Nature *408*, 1004–1008.

Merritt, E.A., and Murphy, M.E.P. (1994). Raster3D version 2.0—a program for photorealistic molecular graphics. Acta Crystallogr. *D50*, 869–873.

Mittl, P.R., Di Marco, S., Krebs, J.F., Bai, X., Karanewsky, D.S., Priestle, J.P., Tomaselli, K.J., and Grutter, M.G. (1997). Structure of recombinant human CPP32 in complex with the tetrapeptide acetyl-Asp-Val-Ala-Asp fluoromethyl ketone. J. Biol. Chem. *272*, 6539–6547.

Morrison, J.F., and Walsh, C.T. (1988). The behavior and significance of slow-binding enzyme inhibitors. Adv. Enz. Relat. Areas Mol. Biol. *59*, 201–301.

Muchmore, S.W., Chen, J., Jakob, C., Zakula, D., Matayoshi, E.D., Wu, W., Zhang, H., Li, F., Ng, S.C., and Altieri, D.C. (2000). Crystal structure and mutagenic analysis of the inhibitor-of-apoptosis protein survivin. Mol. Cell *6*, 173–182.

Navazza, J. (1994). AMoRe: an automated package for molecular replacement. Acta crystallogr. *A50*.

Nicholson, D.W. (1999). Caspase structure, proteolytic substrates, and function during apoptotic cell death. Cell Death Differ. *6*, 1028–1042.

Otwinowski, Z., and Minor, W. (1997). Processing of X-ray diffraction data collected in oscillation mode. Methods Enzymol. *276*, 307–326.

Patston, P.A., Gettins, P., Beecham, J., and Schapira, M. (1991). Mechanism of serpin action: evidence that C1 inhibitor functions as a suicide substrate. Biochemistry USA *30*, 8876–8882.

Read, R.J., and James, M.N.G. (1986). Introduction to the protein inhibitors: x-ray crystallography. In Proteinase Inhibitors, A.J. Barrett, and G. S. Salvesen, eds. (Elsevier Science Publishers BV), pp. 301–336.

Rotonda, J., Nicholson, D.W., Fazil, K.M., Gallant, M., Gareau, Y., Labelle, M., Peterson, E.P., Rasper, D.M., Tuel, R., Vaillancourt, J.P., et al. (1996). The three-dimensional structure of apopain/CPP32, a key mediator of apoptosis. Nat. Struct. Biol. *3*, 619–625.

Roy, N., Deveraux, Q.L., Takahashi, R., Salvesen, G.S., and Reed, J.C. (1997). The c-IAP-1 and c-IAP-2 proteins are direct inhibitors of specific caspases. EMBO J. *16*, 6914–6925.

Rydel, T.J., Ravichandran, K.G., Tulinsky, A., Bode, W., Huber, R., Roitsch, C., and Fenton, J.W. (1990). The structure of a complex of recombinant hirudin and human α-thrombin. Science *249*, 277–280.

Srinivasula, S.M., Datta, P., Fan, X.J., Fernandes-Alnemri, T., Huang, Z., and Alnemri, E.S. (2000). Molecular determinants of the caspase-promoting activity of Smac/DIABLO and its role in the death receptor pathway. J. Biol. Chem. *275*, 36152–36157.

Stennicke, H.R., and Salvesen, G.S. (1999). Caspases: preparation and characterization. Methods *17*, 313–319.

Stennicke, H.R., Jurgensmeier, J.M., Shin, H., Deveraux, Q., Wolf, B.B., Yang, X., Zhou, Q., Ellerby, H.M., Ellerby, L.M., Bredesen, D., et al. (1998). Pro-caspase-3 is a major physiologic target of caspase-8. J. Biol. Chem. *273*, 27084–27090.

Stennicke, H.R., Renatus, M., Meldal, M., and Salvesen, G.S. (2000). Internally quenched fluorescent peptide substrates disclose the subsite preferences of human caspases *1*, 3, *6*, 7 and *8*. Biochem. J. *350*, 563–568.

Stubbs, M.T., Laber, B., Bode, W., Huber, R., Jerala, R., Lenarcic, B., and Turk, V. (1990). The refined 2.4 Å X-ray crystal structure of recombinant human stefin B in complex with the cysteine proteinase papain: a novel type of proteinase inhibitor interaction. EMBO J. *9*, 1939–1947.

Sun, C., Cai, M., Gunasekera, A.H., Meadows, R.P., Wang, H., Chen, J., Zhang, H., Wu, W., Xu, N., Ng, S.C., and Fesik, S.W. (1999). NMR structure and mutagenesis of the inhibitor-of-apoptosis protein XIAP. Nature *401*, 818–822.

Sun, C., Cai, M., Meadows, R.P., Xu, N., Gunasekera, A.H., Herrmann, J., Wu, J.C., and Fesik, S.W. (2000). NMR structure and mutagenesis of the third bir domain of the inhibitor of apoptosis protein XIAP. J. Biol. Chem. *275*, 33777–33781.

Takahashi, R., Deveraux, Q., Tamm, I., Welsh, K., Assa-Munt, N., Salvesen, G.S., and Reed, J.C. (1998). A single BIR domain of XIAP sufficient for inhibiting caspases. J. Biol. Chem. *273*, 7787–7790.

Terwilliger, T.C., and Berendzen, J. (1999). Automated MAD and MIR structure solution. Acta Crystallogr. *D55*, 849–861.

Thornberry, N.A., and Lazebnik, Y. (1998). Caspases: enemies within. Science *281*, 1312–1316.

Thornberry, N.A., Rano, T.A., Peterson, E.P., Rasper, D.M., Timkey, T., Garcia-Calvo, M., Houtzager, V.M., Nordstrom, P.A., Roy, S., Vaillancourt, J.P., et al. (1997). A combinatorial approach defines specificities of members of the caspase family and granzyme B. J. Biol. Chem. *272*, 17907–17911.

Turk, D. (1992). Weiterentwicklung eines Programms fuer Molekuelgraphik und Elektrondichte-Manipulation und seine Anwendung auf verschiedene Protein-Strukturaufklaerungen. (Munich: Technische Universitaet).

Turk, B., Turk, D., and Turk, V. (2000). Lysosomal cysteine proteases: more than scavengers. Biochim Biophys Acta *1477*, 98–111.

Uren, A.G., Coulson, E.J., and Vaux, D.L. (1998). Conservation of baculovirus inhibitor of apoptosis repeat proteins (BIRPs) in viruses, nematodes, vertebrates and yeasts. Trends Biochem. Sci. *23*, 159–162.

Varfolomeev, E.E., Schuchmann, M., Luria, V., Chiannilkulchai, N., Beckmann, J.S., Mett, I.L., Rebrikov, D., Brodianski, V.M., Kemper, O.C., Kollet, O., et al. (1998). Targeted disruption of the mouse Caspase 8 gene ablates cell death induction by the TNF receptors, Fas/Apo1, and DR3 and is lethal prenatally. Immunity *9*, 267–276.

Verdecia, M.A., Huang, H., Dutil, E., Kaiser, D.A., Hunter, T., and Noel, J.P. (2000). Structure of the human anti-apoptotic protein survivin reveals a dimeric arrangement. Nat. Struct. Biol. *7*, 602–608.

Verhagen, A.M., Ekert, P.G., Pakusch, M., Silke, J., Connolly, L.M., Reid, G.E., Moritz, R.L., Simpson, R.J., and Vaux, D.L. (2000). Identification of DIABLO, a mammalian protein that promotes apoptosis by binding to and antagonizing IAP proteins. Cell *102*, 43–53.

Vucic, D., Stennicke, H.R., Pisabarro, M.T., Salvesen, G.S., and Dixit, V.M. (2000). ML-IAP, a novel inhibitor of apoptosis that is preferentially expressed in human melanomas. Curr. Biol. *10*, 1359–1366.

Walker, N.P.C., Talanian, R.V., Brady, K.D., Dang, L.C., Bump, N.J., Ferenz, C.R., Franklin, S., Ghayur, T., Hackett, M.C., Hammill, L.D., et al. (1994). Crystal structure of the cysteine protease interleukin-1beta-converting enzyme: A (p20/p10)2 homodimer. Cell *78*, 343–352.

Watt, W., Koeplinger, K.A., Mildner, A.M., Heinrikson, R.L., Tomasselli, G., and Watenpaugh, K.D. (1999). The atomic resolution structure of human caspase-8, a key activator of apoptosis. Structure *27*, 1135–1143.

Wei, Y., Fox, T., Chambers, S.P., Sintchak, J., Coll, J.T., Golec, J.M., Swenson, L., Wilson, K.P., and Charifson, P.S. (2000). The structures of caspases-1, -3, -7 and -8 reveal the basis for substrate and inhibitor selectivity. Chem. Biol. *7*, 423–432.

Wilson, K.P., Black, J.A., Thomson, J.A., Kim, E.E., Griffith, J.P., Navia, M.A., Murcko, M.A., Chambers, S.P., Aldape, R.A., Raybuck, S.A., and Livingston, D.J. (1994). Structure and mechanism of interleukin-1 beta converting enzyme. Nature *370*, 270–275.

Wu, G., Chai, J., Suber, T.L., Wu, J.W., Du, C., Wang, X., and Shi, Y. (2000). Structural basis of IAP recognition by Smac/DIABLO. Nature *408*, 1008–1012.

Zheng, T.S., Hunot, S., Kuida, K., and Flavell, R.A. (1999). Caspase knockouts: matters of life and death. Cell Death Differ. *6*, 1043–1053.

Zhou, Q., and Salvesen, G.S. (2000). Viral caspase inhibitors CrmA and p35. Methods Enzymol. *322*, 143–154.

Zhou, Q., Snipas, S., Orth, K., Dixit, V.M., and Salvesen, G.S. (1997). Target protease specififfity of the viral serpin CrmA: analysis of five caspases. J. Biol. Chem. *273*, 7797–7800.

Zhou, Q., Krebs, J.F., Snipas, S.J., Price, A., Alnemri, E.S., Tomaselli, K.J., and Salvesen, G.S. (1998). Interaction of the baculovirus anti-apoptotic protein p35 with caspases: specificity, kinetics, and characterization of the caspase/p35 complex. Biochemistry *37*, 10757–10765.

RCSB Accession Code

Coordinates for the caspase-3/BIR2 complex structure have been deposited in the RCSB under the accession code 1I3O.